Optik - International Journal for Light and Electron Optics 207 (2020) 164423

Contents lists available at ScienceDirect

Optik

journal homepage: www.elsevier.com/locate/ijleo

Original research article

Dielectric surface coated with thin partially-reflecting mirror – A revisit to Fresnel laws

Abdel-Baset M.A. Ibrahim[a,*], Hichem Eleuch[b,c], P.K. Choudhury[d], M. Kamil Abd-Rahman[a]

[a] Faculty of Applied Sciences, Universiti Teknologi MARA (UiTM), 40450, Shah Alam, Selangor, Malaysia
[b] Department of Applied Sciences and Mathematics, College of Arts and Sciences, Abu Dhabi University, Abu Dhabi, United Arab Emirates
[c] Institute for Quantum Science and Engineering, Texas A&M University, College Station, Texas, 77843, USA
[d] Institute of Microengineering and Nanoelectronics, Universiti Kebangsaan Malaysia, UKM Bangi, 43600, Selangor, Malaysia

ARTICLE INFO

Keywords:
Optical interaction
Fresnel coefficients
Reflective coating
Geometrical optics

ABSTRACT

New forms of Fresnel reflection and transmission coefficients were derived in the case of oblique optical incidence at the interface of dielectric medium coated with thin partially-reflecting mirror. This essentially required the application of modified boundary conditions for both the electric and magnetic fields. The expressions for power reflectivity (of the mirror) were obtained for both the transverse electric (TE) and transverse magnetic (TM) waves considering the cases of dielectric and metallic coatings. The reflectance and transmittance of the coated surface were also examined corresponding to different values of mirror reflectivity. It is expected that the forms of Fresnel coefficients would be useful in modeling optical and optoelectronic mirror-based devices.

1. Introduction

Fresnel coefficients relate to the reflection and transmission of electromagnetic (EM) waves upon interacting with certain surfaces. These play important roles in the studies of the phenomena of optics and optoelectronics [1–5]. The forms of Fresnel coefficients differ for both the normal and oblique incidence of waves. Furthermore, in the case of oblique incidence, these differ for both the transverse electric (TE) and transverse magnetic (TM) waves [6–9]. In certain optical devices, Fresnel coefficients are utilized to derive the global reflectance and transmittance. In a single layer of an optical medium, the analytical expressions of global reflectance and transmittance can be obtained in terms of Fresnel coefficients. In multilayer structures, these coefficients can be utilized via the transfer matrix method, in order to calculate the global reflectance and transmittance (of the relevant devices).

Fresnel equations are essential in designing many optical components, such as thin-film filters, multi-channel filters, polarizers, and Brewster mirror windows [10–13]. In cavity-based optical devices, such as Fabry-Perot resonators, the optical medium is usually coated with a thin layer of partially-reflecting mirror, in order to control the confinement of light [14–19]. In this case, the most appropriate situation is to derive a new form of Fresnel coefficients where the existence of mirror is taken into account.

In the present work, we derive Fresnel reflection and transmission coefficients for a linear dielectric medium coated with a thin partially-reflecting mirror, considering the oblique incidence of both the TE- and TM-polarized waves. The effect of mirror on Fresnel coefficients and the surface reflectance are investigated for both these polarizations. The derived analytical expressions provide the basis for a reliable description of light wave propagation in photonic devices at oblique incidence, such as Fabry-Perot resonators and

* Corresponding author.
E-mail addresses: abdelbaset@uitm.edu.my, abdelbaset.ibrahim@gmail.com (A.-B.M.A. Ibrahim).

https://doi.org/10.1016/j.ijleo.2020.164423
Received 16 January 2020; Received in revised form 8 February 2020; Accepted 16 February 2020

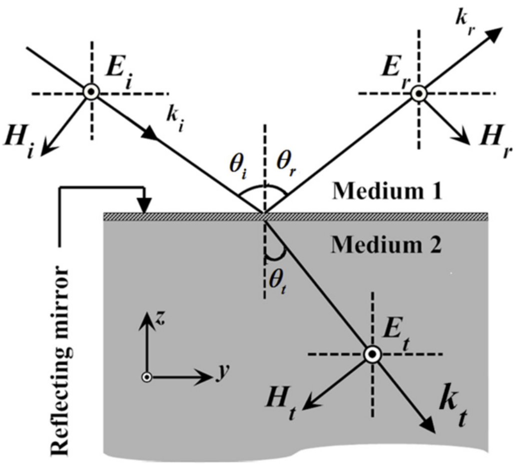

Fig. 1. Schematic of the TE-polarized incidence on a surface of a medium coated with a thin partially-reflecting dielectric mirror.

multilayer structures.

2. Mathematical formulation

Let us consider a situation where the EM wave is obliquely impinged (from free-space) on a linear dielectric medium, as shown in Fig. 1. In oblique incidence, a particular subset of waves may be considered. Here, we consider a TE wave where the electric *E*-field is perpendicular and the magnetic *H*-field is parallel to the plane of incidence. In addition, we consider the case of a TM-polarized wave where the *H*-field is perpendicular and the *E*-field is parallel to the plane of incidence. Mathematically, the EM wave in each medium is described by a plane wave, and then the boundary conditions for both the *E*- and the *H*-fields are applied at the interface. We then solve the resulting equations simultaneously, in order to derive the new forms of Fresnel coefficients. We now consider the two cases individually.

2.1. Case I: TE-Polarized excitation

As shown in Fig. 1, the *E*-field of a TE-polarized wave has one component along the *x*-direction and perpendicular to the *yz*-plane. The EM wave propagates at a fundamental frequencyω relative to a rectangular coordinate system with the base vectors $\hat{i}, \hat{j}, \hat{k}$.

In the medium of incidence (i.e., the Medium 1), the total *E*-field can be written as $\overrightarrow{E_1} = \overrightarrow{E_i} + \overrightarrow{E_r}$, where $\overrightarrow{E_i}$ and $\overrightarrow{E_r}$ are the incident and reflected *E*-fields, respectively. Both $\overrightarrow{E_i}$ and $\overrightarrow{E_r}$ assume the general form of a time-independent plane wave $E_0 exp[i(\overrightarrow{k}.\ \overrightarrow{r})]$ with E_0, $\overrightarrow{k}$ and $\overrightarrow{r}$ being the electric field amplitude, propagation wave vector, and the position vector, respectively. The incident electric field $\overrightarrow{E_i}$ propagates along the wave vector $\overrightarrow{k_i} = k_1 \hat{s}_i$, where k_1 is the wavenumber in the medium of incidence (i.e., the Medium 1) and $\hat{s}_i$ is a unit vector in the direction of $\overrightarrow{k_i}$. The reflected electric field $\overrightarrow{E_r}$ propagates along the wave vector $\overrightarrow{k_r} = k_1 \hat{s}_r$ with $\hat{s}_r$ being a unit vector in the direction of $\overrightarrow{k_r}$. From the geometry of Fig. 1, the wave vectors of the incident and the reflected waves are confined in the *yz*-plane; these can be written as

$$\overrightarrow{k_i} = k_1 \hat{s}_i = sin\theta_i \hat{j} \ - cos\theta_i \hat{k} \tag{1}$$

$$\overrightarrow{k_r} = k_1 \hat{s}_r = sin\theta_r \hat{j} \ + cos\theta_r \hat{k} \tag{2}$$

In Eqs. (1) and (2), θ_i and θ_r are the angle of incidence and reflectance, respectively. In addition, the reflected electric field amplitude E_{0r} is written as $E_{0r} = \rho_{21} E_{0i}$, where ρ_{21} is the Fresnel reflection coefficient. In a similar fashion, the total *H*-field in the medium of incidence (i.e., the Medium 1) is written as $\overrightarrow{H_1} = \overrightarrow{H_i} + \overrightarrow{H_r}$, where $\overrightarrow{H_i}$ and $\overrightarrow{H_r}$ are the incident and the reflected *H*-fields, respectively. In general, for a nonmagnetic medium, the *H*-field can be obtained from the *E*-field using Maxwell's equation $\overrightarrow{H}(r) = [1/i\omega\mu_0]\nabla \times \overrightarrow{E}(r)$, following a standard procedure in the EM theory. Hence, for both the fields in the medium of incidence, we can have

$$\overrightarrow{E_1} = E_0 exp(i\, k_1 y\, sin\theta_i)[exp(-i\, k_1 z\, cos\theta_i) + \rho_{21} exp(i\, k_1 z\, cos\theta_i)]\hat{i} \tag{3}$$

$$\begin{aligned}\overrightarrow{H_1}(y, z) \ &= \frac{k_1 E_{0x}}{\omega\mu_0}\{-[cos\theta_i \hat{j} \ + sin\theta_i \hat{k}\ ]exp(i\, k_1 y\, sin\theta_i - i\, k_1 z\, cos\theta_i)\\ &+\rho_{21}[cos\theta_r \hat{j} \ - sin\theta_r \hat{k}\ ]exp(i\, k_1 y\, sin\theta_r + i\, k_1 z\, cos\theta_r)\}\end{aligned} \tag{4}$$

In the medium of transmittance (i.e., the Medium 2), the transmitted E-field (i.e., $\overrightarrow{E_t}$) assumes a general form of a plane wave with a wave vector $\overrightarrow{k_2} = k_2\hat{s}_t$, where k_2 is the wavenumber in the medium of transmittance and $\hat{s}_t$ is a unit vector in the direction of $\overrightarrow{k_2}$. From the geometry of Fig. 1, we can write the wave vectors of the transmitted wave as

$$\overrightarrow{k_2} = k_2\hat{s}_t = sin\theta_t\hat{j} \; - cos\theta_t\,\hat{k} \tag{5}$$

In Eq. (5), θ_t is the angle of transmittance. The amplitude of the transmitted E-field can also be written as $\tau_{12}E_0$ where τ_{12} is the Fresnel transmission coefficient.

In a similar fashion, we can evaluate the H-field in the medium of transmittance. As such, for both the E- and H-fields in the medium of transmittance, we can write

$$\overrightarrow{E_2}(y, z) = \tau_{12}E_0 exp(i\,k_2 y\,sin\theta_t - i\,k_2 cos\,\theta_t z\,)\hat{i} \tag{6}$$

$$\overrightarrow{H_2}(y, z) \;=\; \frac{-k_2E_{0x}}{\omega\mu_0}\tau_{12}[cos\theta_t\hat{j} \;+ sin\theta_t\hat{k}\;]exp(i\,k_2 y\,sin\theta_t - i\,k_2 z\,cos\theta_t\,) \tag{7}$$

The mirror can be a thin metallic or dielectric layer at the interface between the Mediums 1 and 2. Due to the existence of mirror at the interface, the usual form of boundary conditions are altered, particularly, the continuity of the tangential components of the H-field. In this case, the EM boundary conditions for the tangential components of both the E- and H-fields (i.e., $E^{||}$ and $H^{||}$) can be stated as [14,15,20]

$$(E_1^{||})_{Z=0} = (E_2^{||})_{Z=0}, \quad (H_1^{||} - H_2^{||})_{Z=0} = \eta_M\,(E_{1\,or\,2}^{||})_{Z=0} \tag{8}$$

In Eq. (8), η_M is the mirror coefficient, given as $\eta_M = \sigma_M\delta_M - i\omega\varepsilon_0\varepsilon_M\delta_M$, where$\sigma_M$, δ_M, and ε_M are the mirror conductivity, thickness, and permittivity, respectively. The coefficients ω and ε_0 are the operating angular frequency and free-space permittivity, respectively. The mirror coefficient η_M is complex-valued where the real part represents the metallic contribution, whereas the imaginary part corresponds to the dielectric contribution. The derivation of the previous form of modified boundary conditions is shown in Appendix A.

We now substitute the tangential components of fields from Eqs. (3),(4),(6) and (7) into the boundary conditions in Eq. (8), and solve for ρ_{21} and τ_{12}. In this case, the following expressions for the new Fresnel reflection and transmission coefficients are obtained under the phase-matching conditions:

$$\rho_{21} = \frac{k_1\cos\theta_1 - k_2\cos\theta_t + \alpha_M}{k_1\cos\theta_i + k_2\cos\theta_t - \alpha_M}, \quad \tau_{12} = \frac{2k_1\cos\theta_i}{[k_1\cos\theta_i + k_2\cos\theta_t - \alpha_M]} \tag{9}$$

$$\alpha^M = \omega\mu_0\eta_M = \omega\mu_0\sigma_M\delta_M - i\omega^2\mu_0\varepsilon_0\varepsilon_M\delta_M \tag{10}$$

It should be noted at this point that the boundary conditions for the E-fields under phase-matching conditions necessitate the satisfaction of Fresnel laws of reflection and refraction. That is, $\theta_i = \theta_r = \theta_1$ and $k_1\sin\theta_i = k_2\sin\theta_t$. The dimensional mirror coefficient α^M in Eqs. (9) and (10) is complex with the units of m^{-1}. The former modified coefficients ρ_{21} and τ_{12} in Eqs. (9) and (10) may alternatively be expressed in the terms of refractive index or characteristic impedance, as known in the literature [7,21,22].

$$\rho_{21} = \frac{n_1\cos\theta_i - n_2\cos\theta_t + \alpha_s}{n_1\cos\theta_i + n_2\cos\theta_t - \alpha_s}, \quad \tau_{12} = \frac{2n_1\cos\theta_i}{n_1\cos\theta_i + n_2\cos\theta_t - \alpha_s} \tag{11}$$

$$\alpha_s = \alpha_a - i\alpha_b = c\mu_0\sigma_M\delta_M - i\left(\frac{\omega}{c}\right)\varepsilon_M\delta_M \tag{12}$$

In these equations, α_s is the scaled form of the mirror coefficient α_M wherein α_a and α_b are, respectively, the real and imaginary parts.

As α_s does not have a very direct physical significance, it is then important to derive a relationship between α_s and the power reflectivity of R_M of the coating mirror at the interface under linear approximation. To do so, we use $R_M = \rho_{21}\rho_{21}^*$ (with ρ_{21}^* being the complex conjugate of ρ_{21}). This leads to the following equations for R_M:

$$R_M = \frac{(n_1\cos\theta_i - n_2\cos\theta_t\,)^2 + (\alpha_s^* + \alpha_s)(n_1\cos\theta_i - n_2\cos\theta_t\,) + \alpha_s\alpha_s^*}{(n_1\cos\theta_i + n_2\cos\theta_t)^2 - (\alpha_s^* + \alpha_s)(n_1\cos\theta_i + n_2\cos\theta_t\,) + \alpha_s\alpha_s^*} \tag{13}$$

For a pure dielectric mirror, where the metallic conductivity $\sigma_M \to 0$, the term $\alpha_a \to 0$, and α_s reduces to– $i\alpha_b = -i\omega\varepsilon_M\delta_M/c$. In the case of an ideal metallic mirror, the dielectric permittivity of the mirror material $\varepsilon_M \to 0$, the term $\alpha_b \to 0$, and α_s reduces to $\alpha_s = \alpha_a = c\mu_0\sigma_M\delta_M$ [20]. Consequently, Eq. (13) splits to the following two equations for the dielectric and metallic mirrors:

$$R_{M,TE\text{›}Dielectric} = \frac{(n_1\cos\theta_i - n_2\cos\theta_t\,)^2 + \alpha_b^2}{(n_1\cos\theta_i + n_2\cos\theta_t)^2 + \alpha_b^2} \tag{14}$$

$$R_{M,TE\text{›}Metallic} = \frac{[(n_1\cos\theta_i - n_2\cos\theta_t\,) + 2\alpha_a](n_1\cos\theta_i - n_2\cos\theta_t\,) + \alpha_a^2}{[(n_1\cos\theta_i + n_2\cos\theta_t) - 2\alpha_a](n_1\cos\theta_i + n_2\cos\theta_t) + \alpha_a^2} \tag{15}$$

Exploiting these equations, we can find the corresponding reflectivity $R_{M,TE}$ of the mirror for each value of the mirror coefficient α_s in the case of a TE-polarized wave.

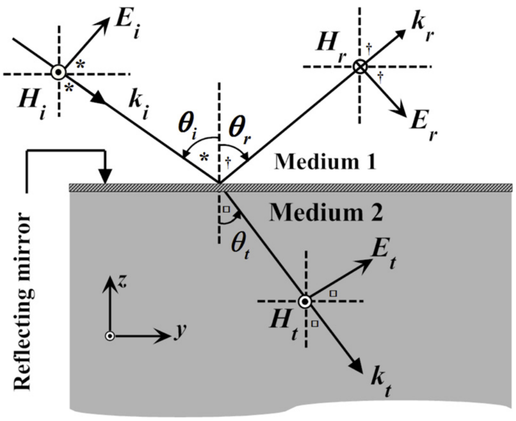

Fig. 2. Schematic of the TM-polarized incidence on a surface of a medium coated with a thin partially-reflecting dielectric mirror.

2.2. Case II: TM-Polarized excitation

As in the previous section, the incident and reflected electric fields for the TM-polarized wave also assume the general form of a uniform time-independent plane wave. As shown in Fig. 2, the incident electric field $\overrightarrow{E_i}$ propagates along the wave vector $\overrightarrow{k_i} = k_1\hat{s_i}$, where k_1 is the wavenumber in the medium of incidence (i.e., the Medium 1) and $\hat{s_i}$ is a unit vector in the direction of $\overrightarrow{k_i}$.

From the geometry of Fig. 2, we may write $\hat{s_i} = sin\,\theta_i\hat{j} - cos\,\theta_i\,\hat{k}$. However, for a TM wave, the E-field points towards an arbitrary direction relative to the Cartesian coordinate system. Hence, $\overrightarrow{E_i} = E_0\hat{e_i}$, where E_0 is the incident E-field amplitude and $\hat{e_i}$ is a unit vector pointing towards the arbitrary direction of $\overrightarrow{E_i}$. Fig. 2 also allows to write $\hat{e_i} = cos\,\theta_i\hat{j} + sin\,\theta_i\,\hat{k}$. In a similar fashion, the reflected electric field $\overrightarrow{E_r}$ has the amplitude E_0 pointing along $\hat{e_r}$ where $\hat{e_r} = cos\,\theta_r\hat{j} - sin\,\theta_r\,\hat{k}$, and propagates along the wave vector $\overrightarrow{k_r} = k_1\hat{s_r}$ with $\hat{s_r} = sin\,\theta_r\hat{j} + cos\,\theta_r\hat{k}$. However, the application of boundary conditions requires only the tangential components of both the E- and H-fields. Therefore, the tangential components for EM field in the Medium 1 can be written as

$$E_{1,||} = E_0\cos\theta_i\exp[ik_1(y\sin\theta_i - z\cos\theta_i)] + E_0\rho_{21}\cos\theta_r\exp[ik_1(y\sin\theta_i + z\cos\theta_i)] \tag{16}$$

$$H_{1,||} = \frac{E_0k_1}{\omega\mu_0}\{\exp[ik_1(y\sin\theta_i - z\cos\theta_i)] - \rho_{21}\exp[ik_1(y\sin\theta_i + z\cos\theta_i)]\} \tag{17}$$

With reference to the geometry of Fig. 2, the y-component of the transmitted electric field $\overrightarrow{E_t}$ and the corresponding magnetic field in the Medium 2 may also be written in the following form:

$$E_{2,||}(y,z) = \tau_{12}E_0\cos\theta_t\exp[ik_2(y\sin\theta_t - z\cos\theta_t)] \tag{18}$$

$$H_{2,||} = \frac{\tau_{12}E_0}{\omega\mu_0}k_2\exp[ik_2(y\sin\theta_t - z\cos\theta_t)] \tag{19}$$

Similar to the previous section, we substitute the tangential field components from Eqs. (16)—(19) into the boundary conditions in Eq. (8), and then solve the system simultaneously under the phase-matching conditions. After some mathematical steps; we finally obtain the following expressions:

$$\rho_{21} = \frac{k_1\cos\theta_t - k_2\cos\theta_i - \alpha_M\cos\theta_i\cos\theta_t}{k_1\cos\theta_t + k_2\cos\theta_i + \alpha_M\cos\theta_i\cos\theta_t} = \frac{n_1\cos\theta_t - n_2\cos\theta_i - \alpha_s\cos\theta_i\cos\theta_t}{n_1\cos\theta_t + n_2\cos\theta_i + \alpha_s\cos\theta_i\cos\theta_t} \tag{20}$$

$$\tau_{12} = \frac{2k_1\cos\theta_i}{k_1\cos\theta_t + k_2\cos\theta_i + \alpha_M\cos\theta_i\cos\theta_t} = \frac{2n_1\cos\theta_i}{n_1\cos\theta_t + n_2\cos\theta_i + \alpha_s\cos\theta_i\cos\theta_t} \tag{21}$$

Eqs. (20) and (21), respectively, describe the Fresnel reflection and transmission coefficients in the case of TM-polarized wave.

In the former equations, the mirror parameters α_M and α_s remain as in the previous case corresponding to the TE-polarized incidence. In this case, the mirror reflectivity $R_{M,TM} = \rho_{21,TM}\rho^*_{21,TM}$ of the TM wave can be written as

$$R_{M,TM} = \frac{[(n_1\cos\theta_t - n_2\cos\theta_i)^2 - (\alpha_s^* + \alpha_s)\cos\theta_i\cos\theta_t(n_1\cos\theta_t - n_2\cos\theta_i) + |\alpha_s|^2\cos^2\theta_i\cos^2\theta_t]}{[(n_1\cos\theta_t + n_2\cos\theta_i)^2 + (\alpha_s^* + \alpha_s)\cos\theta_i\cos\theta_t(n_1\cos\theta_t + n_2\cos\theta_i) + |\alpha_s|^2\cos^2\theta_i\cos^2\theta_t]} \tag{22}$$

Eq. (22) can also be used to obtain the reflectivity of both the cases of dielectric and metallic mirrors for the TM-polarized wave. Finally, the respective equations are as follows:

$$R_{M,TM})_{Dielectric} = \frac{(n_1\cos\theta_t - n_2\cos\theta_i)^2 + \alpha_b^2\cos^2\theta_i\cos^2\theta_t}{(n_1\cos\theta_t + n_2\cos\theta_i)^2 + \alpha_b^2\cos^2\theta_i\cos^2\theta_t} \tag{23}$$

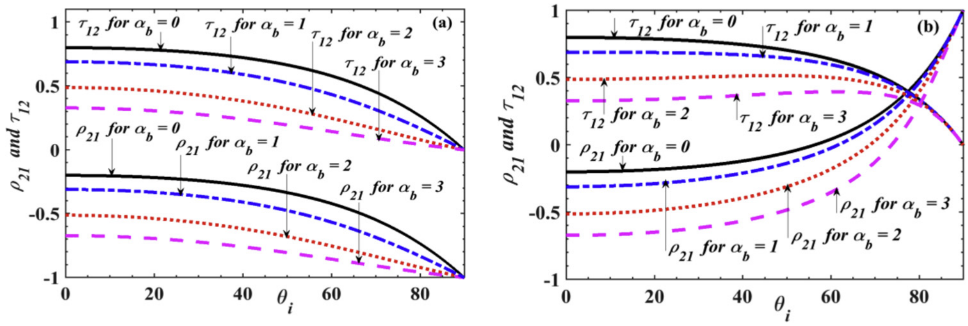

Fig. 3. Plots of Fresnel reflection and transmission coefficients of the surface medium vs. the angle of incidence at different values of mirror reflectivity in the cases of (a) TE- and (b) TM-polarized incidence excitations.

$$R_{M,TM})_{Metallic} = \frac{(n_1\cos\theta_t - n_2\cos\theta_i)^2 - 2\alpha_a\cos\theta_i\cos\theta_t(n_1\cos\theta_t - n_2\cos\theta_i) + \alpha_a^2\cos^2\theta_i\cos^2\theta_t}{(n_1\cos\theta_t + n_2\cos\theta_i)^2 + 2\alpha_a\cos\theta_i\cos\theta_t(n_1\cos\theta_t + n_2\cos\theta_i) + \alpha_a^2\cos^2\theta_i\cos^2\theta_t} \quad (24)$$

Eqs. (23) and (24) describe the reflectivity of partially-reflecting dielectric and metallic mirrors, respectively, placed at the surface of a linear dielectric medium. Similar to Eqs. (14) and (15), Eqs. (23) and (24) draw a direct connection between the mirror coefficient α_b and the corresponding mirror reflectivity R_M for both the TE- and TM-polarized waves at different angles of incidence.

3. Discussion

In the following section, we discuss the implication of the existence of mirrors on the reflection coefficients. In Fig. 3, we plot the reflection and transmission coefficients of the dielectric medium in the cases of both the TE- and TM-polarized incidence excitations, whereas in Fig. 4, we plot the surface reflectance R and transmittance T using the same parameters, as in Fig. 3.

In Figs. 3 and 4 both, the solid curves represent the usual case without utilizing a mirror (i.e., $\alpha_b = 0$), while in other curves, the mirror coefficient increases gradually. The family of curves with the value of α_b as 1, 2 and 3 maintain the typical behavior for both the TE- and TM-polarized waves. For example, the relation $R + T = 1$ holds for all curves. In addition, for the TE-polarized incidence, the reflectance increases gradually with increasing θ_i, while the transmittance T decreases. However, in the case of TM wave incidence, the reflectance decreases first, reaches a minimum value, and increases thereafter.

For the TM-polarized excitation, without a mirror, the reflectance reaches zero at Brewster angle θ_B. However, when $\alpha_b \neq 0$, Brewster angle disappears even when the reflectance reaches the minimum. This seems natural when the surface is coated with a dielectric mirror with a slightly different dielectric permittivity, since the mirror always reflects a specific portion of light. In addition, a shift in the minimum value of R or the maximum value of T occurs at higher values of θ_i.

At normal incidence (i.e., $\theta_i = 0$), for both the TE- and TM-polarized waves, the reflectivity R of the coated surface increases with the increase in mirror reflectivity R_M. For example, for the cases of TE and TM waves both, the surface reflectivity is 17% when $\alpha_b = 1$. Corresponding to $\alpha_b = 2$, the surface reflectivity increases to 41%, and at $\alpha_b = 2$, it becomes 61%.

In general, at any value of θ_i, the surface reflectivity is elevated because of the mirror, and this elevation depends on the mirror confect or reflectivity. It is also interesting to note that, the reflectance and transmittance of the surface become equal at a specific angle of incidence. Here, for the TE-polarized wave, at $\alpha_b = 0$, $R = T$ at $\theta_i = \theta_e \approx 79^o$. With the existence of mirror, this angle of equal reflectance and transmittance is shifted to $\theta_e \approx 70^o$ for $\alpha_b = 1$, and $\theta_e \approx 38^o$ for $\alpha_b = 2$. However, no intersection between R and T occurs at $\alpha_b = 3$, as shown in Fig. 4a. For the TM-polarized wave, the angle of equal reflectance and transmittance θ_e occurs at $\theta_e \approx 79^o$for all values of α_b, i.e., $\alpha_b = 0,\ 1,\ 2,$ and 3. Interestingly, for $\alpha_b = 3$, the situation of $R = T$ occurs at $\theta_e = 42^0$ as well.

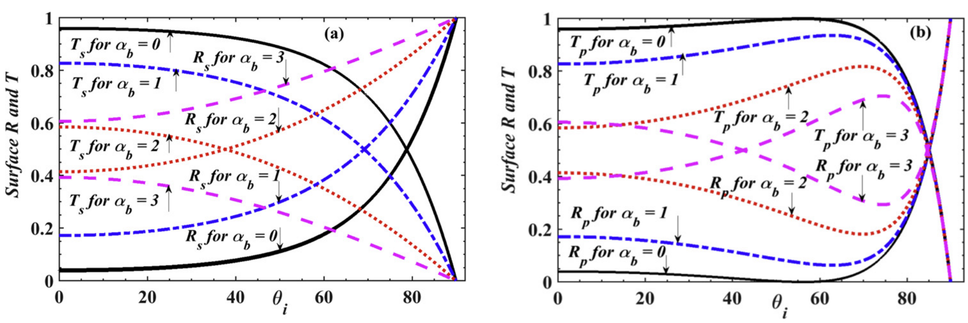

Fig. 4. Plots of reflectance and transmittance of the medium vs. the angle of incidence at different values of mirror reflectivity in the cases of (a) TE- and (b) TM-polarized incidence excitations.

4. Conclusion

New forms of Fresnel reflection and transmission coefficients at the interface of a dielectric medium, coated with a thin partially-reflecting mirror, are developed at the oblique incidence of the TE- and TM-polarized excitations. With the existence of a thin partially reflecting mirror, these coefficients contain a complex-valued mirror parameter $\alpha = \alpha_a - i\alpha_b$, the real part of which represents a metallic coating of mirror material, whereas the imaginary part the dielectric mirror coating. For pure metallic coating, the mirror parameter α_a is a function of its thickness δ_M and conductivity σ_M, whereas for pure dielectric coating, the mirror parameter α_b is a function of its thickness δ_M and the dielectric permittivity ε_M. The expressions for power reflectivity R_M of the mirror coating for both the TE- and TM-polarized excitations for the dielectric as well as metallic coatings are also derived. With these expressions, a direct relationship between the power reflectivity of mirror and the mirror parameter could be established. The reflectivity of mirror coating is found to be the functions of mirror parameter, angle of incidence, angle of transmittance, and the refractive index of both the incidence and transmitting mediums.

The features of this new form of Fresnel coefficients (ρ_{21}, τ_{12}), and the corresponding reflectance and transmittance (R, T) of surface, are also examined for different values mirror reflectivity. The obtained results provide a proper form of Fresnel coefficients for the modeling of mirror-based devices, such as Fabry-Perot resonators and multilayer structures.

Funding information

AMAI acknowledges the financial support by the Universiti Teknologi MARA (UiTM) through the grant number 600-IRMI/5/3/GIP(001/2018). Also, PKC acknowledges the grant FRGS/1/2019/STG02/UKM/01/1 by the Ministry of Higher Education (MOHE), Malaysia toward research support.

Declaration of Competing Interest

None.

Appendix A

Boundary conditions at the interface between two mediums separated by thin coating mirror [14,15,20]

Let us consider two mediums, identified by the dielectric permittivity values ε_1, ε_2, are separated at the boundary by a thin (metallic or dielectric) mirror of thickness δ_M, dielectric permittivity ε_M, and conductivity σ_M. We apply the boundary conditions at the interface to an infinitesimal volume element positioned with its *upper-half* lying in the Medium 1 and the *lower-half* in the Medium 2. As stated, both the mediums are separated by a thin mirror, as shown in the Fig. A1.

The first boundary condition for the electric E-field is obtained upon applying the Maxwell-Faraday law to the contour *abcd*, i.e.,

(A.1)$\oint_c \vec{E}\,.\,d\vec{l} = \frac{d}{dt}\int_s \vec{B}\,.\,d\vec{s}$

The direction of contour integral c follows the right-hand rule with the unit normal, as in the diagram. The magnetic flux $\int_s \vec{B}\,.\,d\vec{s} = 0$ is based on the Gauss law of magnetic field. Therefore, we obtain

(A.2)$\oint_c \vec{E}\,.\,d\vec{l} = E_{2t}\Delta y - E_{1t}\Delta y = 0$

As such, we can have

(A.3)$E_{2t} = E_{1t}$

The second boundary condition corresponding to the magnetic H-field is obtained upon using the Maxwell-Ampere law

(A.4)$\oint_c \vec{H}\,.\,d\vec{l} = -i\omega\int_s \vec{D}\,.\,d\vec{s} + \int_s \vec{J}\,.\,d\vec{s}$

As for the electric flux density, in the case without a mirror, the rectangle sides Δz perpendicular to the boundary are allowed to

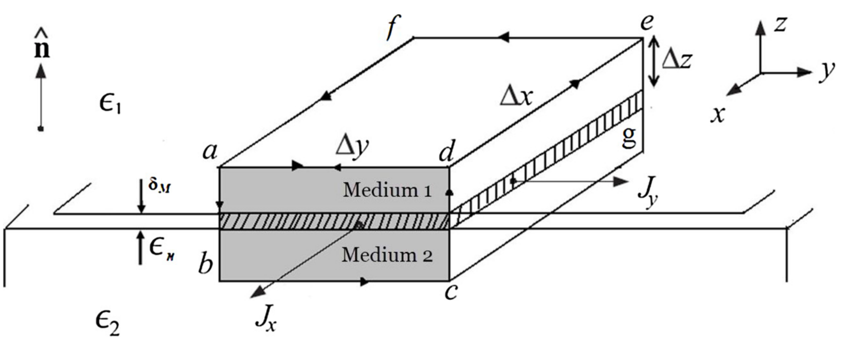

Fig. A1. Infinitesimal volume element with its upper-half in the medium 1 and the lower-half in the medium 2; the two mirrors being separated by a very thin coating mirror in the middle.

shrink to zero. Therefore, the electric flux density $\frac{d}{dt}\int_s \overrightarrow{D}\,.\,\overrightarrow{ds} = 0$ and the current flux density $\int_s \overrightarrow{J}\,.\,\overrightarrow{ds} = 0$ cutting the loop are allowed to shrink to zero. However, when a thin mirror is placed at the boundary, the electric flux density and current flux density shrink to a small area with length Δy and thickness $\Delta z = \delta_M$. In this case, Eq. (A.4) reduces to the following form:

(A.5)$H_{2t}\Delta y - H_{1t}\Delta y = -i\omega(D_{n,M}\Delta y\delta_M) + J_{n,M}\Delta y\delta_M$

In the linear régime, $D_{n,M} = \varepsilon_0\varepsilon_M E_{n,M}$ and $J_{n,M} = \sigma_M E_{n,M}$; this gives

(A.6)$H_{2t} - H_{1t} = -i\omega\varepsilon_0\varepsilon_M\delta_M E_{n,M} + \sigma_M\delta_M E_{n,M}$

Therefore, the application of boundary conditions on the face *abcd* gives the following:

(A.7)$E_{1y} = E_{2y}, \quad H_{2y} - H_{1y} = \eta_M E_{1x\ or\ 2x}, \ \ \eta_M = \sigma_M\delta_M - i\omega\varepsilon_0\varepsilon_M\delta_M$

As seen in Eq. (A.7), the field inside the mirror can either be represented by the field in the Medium 1 or the Medium 2. In a similar fashion, if we apply the boundary conditions on the other contour *edcg*, we obtain

(A.8)$E_{1x} = E_{2x}, \quad H_{1x} - H_{2x} = \eta_M E_{1y\ or\ 2y}$

The difference in the sign of magnetic field in both the equations results from the direction of line integral, which has to follow the right-hand rule with the net flux pointing outward.

References

[1] S. Luhn, M. Hentschel, Analytical Fresnel laws for curved dielectric interfaces, J. Opt. 22 (1) (2019) 015605.
[2] M. Hentschel, H. Schomerus, Fresnel laws at curved dielectric interfaces of microresonators, Phys. Rev. E 65 (4) (2002) 045603.
[3] M.R. Chatterjee, N. Buaossa, Planar electromagnetic propagation of an s-polarized wave across an achiral/chiral interface under variable magnetic permeability, Front. Optics Optic. Soc. Am. (2019) pp. JW3A–111..
[4] R. Y. Ataai and M. R. Chatterjee, Electromagnetic reflection and transmission response of a chiral slab resonator to a circularly polarized wave, in 2019 IEEE Photonics Conference (IPC) (IEEE, n.d.), pp. 1–2.
[5] R.Y. Ataai, M.R. Chatterjee, Propagation of a left-circularly polarized electromagnetic wave through a chiral slab resonator based on Fresnel coefficients, Front. Optics Optic. Soc. Am. (2019) pp. JW4A–23.
[6] M. Born, E. Wolf, Principles of Optics: Electromagnetic Theory of Propagation, Interference and Diffraction of Light, Cambridge University Press, 1999.
[7] O.S. Heavens, Optical Properties of Thin Solid Films, Dover Publications, INC, 1991.
[8] K. Zhang, D. Li, K. Chang, K. Zhang, D. Li, Electromagnetic Theory for Microwaves and Optoelectronics, Springer-Verlag, 1998.
[9] P. Yeh, Optical Waves in Layered Media, Wiley, 2005.
[10] B.E. Saleh, M.C. Teich, Fundamentals of Photonics, John Wiley & Sons, 2019.
[11] M.A. Baqir, P.K. Choudhury, T. Fatima, A.-B. Ibrahim, Graphene-over-graphite-based metamaterial structure as optical filter in the visible regime, Optik 180 (2019) 832–839.
[12] N. Iqbal, P.K. Choudhury, Mode filtering aspects of periodic multilayered chiro-ferrite medium, Optik 157 (2018) 449–454.
[13] S. Moghaddas, M. Ghasemi, P.K. Choudhury, B.Y. Majlis, Engineered metasurface of gold funnels for terahertz wave filtering, Plasmonics 13 (5) (2018) 1595–1601.
[14] A.-B.M.A. Ibrahim, D.R. Tilley, J. Osman, Optical bistability from ferroelectric Fabry-Pérot interferometer, Ferroelectrics 355 (1) (2007) 140–144.
[15] S.-C. Lim, J. Osman, D.R. Tilley, The gyromagnetic Fabry-Pérot resonator: II. Dipole-exchange effects, J. Phys. Condens. Matter 10 (8) (1998) 1891.
[16] R. Murgan, F. Razak, D.R. Tilley, T.Y. Tan, J. Osman, M.N.A. Halif, Second harmonic generation from a ferroelectric film, Comput. Mater. Sci. 30 (3–4) (2004) 468–473.
[17] M.N.A. Halif, S. Daud, J. Osman, Oscillatory dynamical switching system of bulk ferroelectrics, Am. J. Appl. Sci. 2 (6) (2005) 1073–1077.
[18] M.N.A. Halif, D.R. Tilley, K.H. Chew, J. Osman, Reflection and transmission of ferroelectric materials in the first-order phase transition, J. Fiz. Malays 25 (1 & 2) (2004) 23–28.
[19] J. Osman, K.H. Chew, Y. Ishibashi, D.R. Tilley, M.N.A. Halif, Surface modification of bulk state for the first-order ferroelectric phase transition, J. Fiz. Malays 25 (3 & 4) (2004) 137–139.
[20] K.-H. Chew, J. Osman, D.R. Tilley, The nonlinear Fabry–Pérot resonator: direct numerical integration, Opt. Commun. 191 (3–6) (2001) 393–404.
[21] R.A. Chipman, W.S.T. Lam, G. Young, Polarized Light and Optical Systems, CRC Press, 2018.
[22] P. Baumeister, Optical Coating Technology, SPIE press, 2004, p. 137.